

## Vertical distributions of lateral forces on base isolated structures considering higher mode effects

C. S. Tsai<sup>†</sup>

*Department of Civil Engineering, Feng Chia University, Taichung, Taiwan, ROC*

Wen-Shin Chen<sup>‡</sup>

*Graduate Institute of Civil and Hydraulic Engineering, Feng Chia University, Taichung, Taiwan, ROC*

Bo-Jen Chen<sup>‡†</sup>

*R&D Department, Earthquake Proof System, Inc., Taichung, Taiwan, ROC*

Wen-Shen Pong<sup>‡‡</sup>

*School of Engineering, San Francisco State University, USA*

*(Received November 28, 2005, Accepted March 30, 2006)*

**Abstract.** Base isolation technology has been accepted as a feasible and attractive way in improving seismic resistance of structures. The seismic design of new seismically isolated structures is mainly governed by the Uniform Building Code (UBC-97) published by the International Conference of Building Officials. In the UBC code, the distribution formula of the inertial (or lateral) forces leads to an inverted triangular shape in the vertical direction. It has been found to be too conservative for most isolated structures through experimental, computational and real earthquake examinations. In this paper, four simple and reasonable design formulae, based on the first mode of the base-isolated structures, for the lateral force distribution on isolated structures have been validated by a multiple-bay three-story base-isolated steel structure tested on the shaking table. Moreover, to obtain more accurate results for base-isolated structures in which higher mode contributions are more likely expected during earthquakes, another four inertial force distribution formulae are also proposed to include higher mode effects. Besides the experimental verification through shaking table tests, the vertical distributions of peak accelerations computed by the proposed design formulae are in good agreement with the recorded floor accelerations of the USC University Hospital during the Northridge earthquake.

**Keywords:** base isolation; structural control; UBC code; lateral force distribution; higher mode effect.

---

<sup>†</sup> Professor, Corresponding author, E-mail: [cstai@fcu.edu.tw](mailto:cstai@fcu.edu.tw)

<sup>‡</sup> Ph. D. Student

<sup>‡†</sup> Ph. D., Assistant Research Fellow

<sup>‡‡</sup> Associate Professor

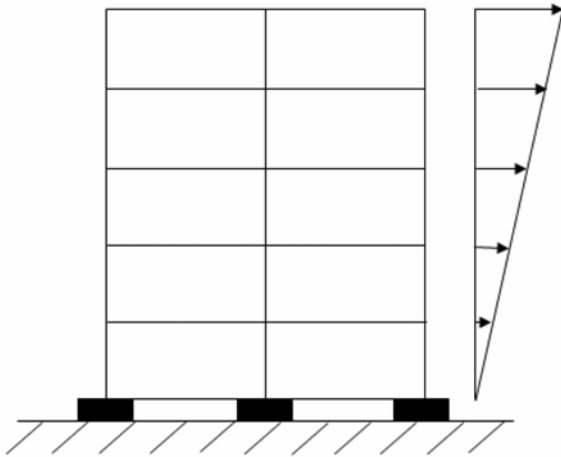


Fig. 1 Vertical distributions of inertia forces suggested in UBC code provision for base isolation system

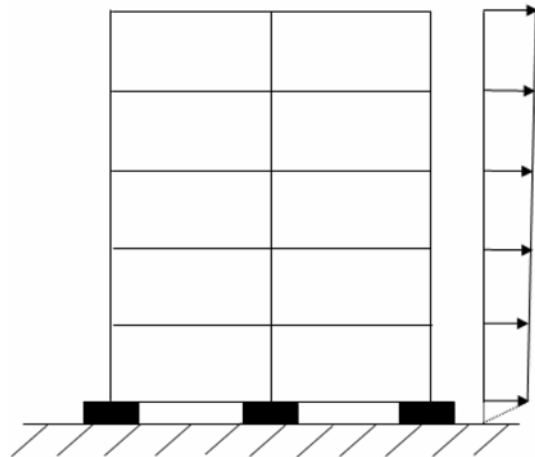


Fig. 2 Vertical distributions of inertia forces suggested in proposed design formulae for base isolation system

## 1. Introduction

Base isolation is an innovative seismic design approach in which flexible elements are implemented in the foundation of a structure to lengthen the natural period of a structure and to reduce the transmission of energy from the ground into the structure. In recent years, the effectiveness of base isolation systems has been demonstrated through destructive seismic events, and the base isolation of the primary structure has become crucial to protect both structural and nonstructural components from strong earthquake impacts. Meanwhile, the interrelated building codes and technical specifications for base-isolated structures have been revealed to accelerate their applications in the engineering community.

The design of seismically isolated structures in the United States are currently governed by the Uniform Building Code published by the International Conference of Building Officials (ICBO), and the National Earthquake Hazards Reduction Program (NEHRP) Guidelines for the Seismic Rehabilitation of Buildings (FEMA-273) and its commentary (FEMA-274) which were published by the Federal Emergency Management Agency (Uniform Building Code 1997, FEMA-273 1993, FEMA-274 1994). The distribution of lateral design forces over the height of the superstructure proposed in the UBC-97 and FEMA-273 is on the basis of an inverted triangular distribution that is generally used for fixed-base structures, as shown in Fig. 1. In recent years, this distribution of inertial (or lateral) forces over the height of the superstructure above isolation has been found to bound responses of most isolated structures conservatively. Tsai *et al.* (2001a,b, 2002a, 2003a), analytically based on the first mode of the base-isolated structure without complex calculation, have proposed two simple and reasonable design formulae for the lateral force distribution on an isolated structure. These two proposed design formulae can accurately predict the lateral force distributions on isolated structures via the computational validation and experimental verification of a full-scale isolated structure tested on the shaking table (Tsai *et al.* 2001a,b, 2002a, 2003a). As shown in Fig. 2, these two proposed design formulae assume that the vertical distribution of inertia forces on an

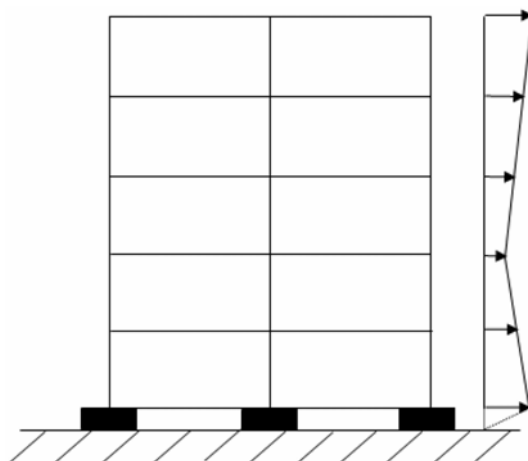


Fig. 3 Vertical distributions of inertia forces suggested in proposed design formulae considering higher mode effects for base isolation system

isolated structure should be the first mode of the base-isolated structure rather than an inverted triangular force distribution suggested by the UBC code. Furthermore, in the UBC code, the weight of the base floor is ignored, which will overestimate the inertial force and maximum absolute acceleration on each floor. The proposed design formulae by Tsai *et al.* (2001a,b, 2002a, 2003a) also reasonably incorporate the influence of the inertial force on the base floor to calculate accurately the vertical distribution of inertial forces on a base-isolated structure. Lee *et al.* (2001) also proposed a formula derived by combining the fundamental mode shape of the isolated structure idealized as two degrees of freedom system and the fundamental mode shape of a fixed-based structure to compute the vertical distribution of seismic load. However, the above-mentioned methods may not be applicable for the irregular or high-rise buildings in which higher mode responses are significant.

In this paper, to obtain more accurate results for base-isolated structures in which higher mode responses are expected during earthquakes, as shown in Fig. 3, there are another four inertial force distribution formulae proposed by considering higher modes of the base-isolated structures and the superstructures based on the theory of structural dynamics (Kelly 1997, Naeim and Kelly 1999, Kelly 1999, Chopra 1995, Chopra and Goel 2002, Jan *et al.* 2002). The effects of the first two modes of the base-isolated structure and the superstructure are included to improve accuracy of the lateral force distribution without surrendering simplicity (Tsai *et al.* 2003b, Chen 2003).

To compare the lateral force distributions computed from the proposed design formulae and UBC code provision, the experimental verification of a multiple-bay base-isolated steel structure in the shaking table tests at the National Center for Research on Earthquake Engineering in Taiwan has been carried out. Besides the experimental verification through shaking table tests, the recorded floor accelerations of the USC University Hospital during the Northridge earthquake were also adopted to investigate the suitability of the proposed design formulae considering higher mode effects in this paper. It is illustrated from comparison results that the proposed design formulae can well predict the vertical distributions of lateral forces on isolated structures during earthquakes, and that the lateral force distributions calculated by the UBC code are too conservative. Moreover, it will obtain more satisfactory results by considering the contributions of higher modes for irregular base-isolated structures.

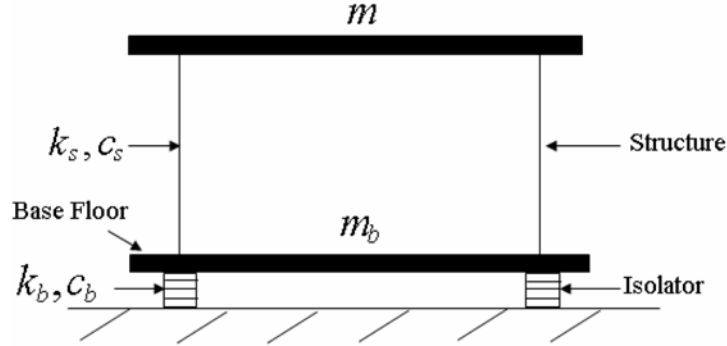


Fig. 4 Two-degree-of-freedom base isolation system

## 2. Linear theory of base-isolated structures

In order to gain insight into the behavior of base-isolated structures, the linear theory of base isolation has already been developed by J. M. Kelly using a simple 2-DOF model with linear spring and linear viscous damping (Kelly 1997, Naeim and Kelly 1999, Kelly 1999). As shown in Fig. 4, one is the degree of freedom of the superstructure, and the other is the degree of freedom of the base isolator.

In most structural applications it is assumed that the damping is small enough and that effect of the off-diagonal components is negligible. The equations of motions are written by (Kelly 1997, Naeim and Kelly 1999, Kelly 1999):

$$\ddot{q}_1 + 2\omega_1\beta_1\dot{q}_1 + \omega_1^2q_1 = -L_1\ddot{u}_g \quad (1)$$

and

$$\ddot{q}_2 + 2\omega_2\beta_2\dot{q}_2 + \omega_2^2q_2 = -L_2\ddot{u}_g \quad (2)$$

where  $q_1$  and  $q_2$  are time-dependent modal coefficients;  $\ddot{u}_g$  denotes the absolute acceleration of the ground. The analytical solution of natural frequencies and damping ratios of the base-isolated structure can be given by:

$$\omega_1^2 = \omega_b^2(1 - \gamma\varepsilon), \quad \omega_2^2 = \frac{\omega_s^2}{1 - \gamma}(1 + \gamma\varepsilon) \quad (3)$$

and

$$\beta_1 = \beta_b\left(1 - \frac{3}{2}\gamma\varepsilon\right), \quad \beta_2 = \left[\frac{\beta_s + \gamma\beta_b\varepsilon^{1/2}}{(1 - \gamma)^{1/2}}\right]\left(1 - \frac{1}{2}\gamma\varepsilon\right) \quad (4)$$

where

$$\omega_b = \sqrt{\frac{k_b}{(m + m_b)}}, \quad \omega_s = \sqrt{\frac{k_s}{m}} \quad (5)$$

and

$$\beta_b = \frac{c_b}{2(m + m_b)\omega_b}, \quad \beta_s = \frac{c_s}{2m\omega_s} \quad (6)$$

Two important parameters are defined as

$$\varepsilon = \frac{\omega_b^2}{\omega_s^2}, \quad \gamma = \frac{m}{m + m_b} \quad (7)$$

where  $m$  and  $m_b$  represent the mass of the superstructure (i.e., without base slab) and the mass of the base floor, respectively;  $c_b$  and  $k_b$  are the linear viscous damping coefficient and effective stiffness of the base isolator, respectively;  $c_s$  and  $k_s$  depict the damping coefficient and stiffness of the superstructure, respectively.

The participation factors,  $L_1$  and  $L_2$ , for the first two modes in these equations are given by

$$L_1 = 1 - \gamma\varepsilon, \quad L_2 = \gamma\varepsilon \quad (8)$$

Then, the maximum values of  $q_1$  and  $q_2$  can be given by

$$|q_1|_{\max} = L_1 S_D(\omega_1, \beta_1), \quad |q_2|_{\max} = L_2 S_D(\omega_2, \beta_2) \quad (9)$$

where  $S_D(\omega, \beta)$  is the displacement response spectrum for the ground motion,  $\ddot{u}_g$ , at frequency  $\omega$  and damping ratio  $\beta$ .

Moreover, the mode shapes are given by:

$$\phi^1 = \begin{Bmatrix} 1 \\ \varepsilon \\ 1 - \gamma\varepsilon \end{Bmatrix}, \quad \phi^2 = \begin{Bmatrix} 1 \\ 1 + \gamma\varepsilon \\ -\gamma(1 + \varepsilon) \end{Bmatrix} \quad (10)$$

If  $\gamma\varepsilon \ll 1$ , Eq. (10) can be rewritten as (Kelly 1997, Naeim and Kelly 1999, Kelly 1999):

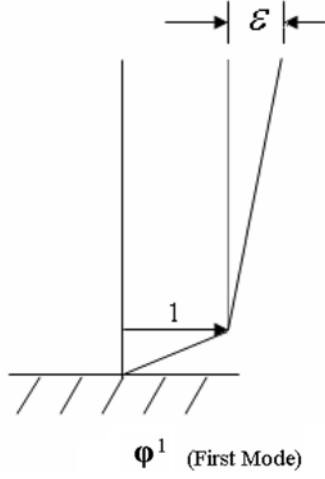
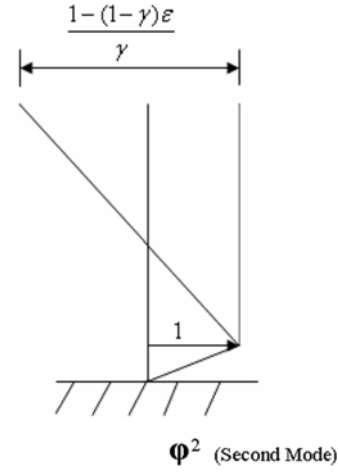
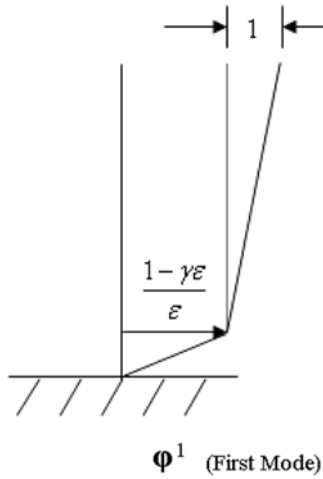
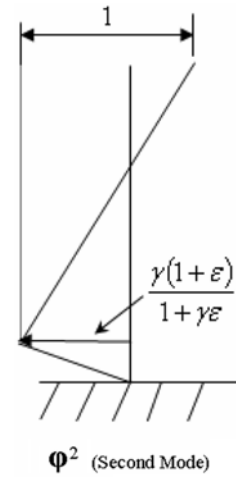
$$\phi^1 = \begin{Bmatrix} 1 \\ \varepsilon \end{Bmatrix}, \quad \phi^2 = \begin{Bmatrix} 1 \\ -\frac{[1 - (1 - \gamma)\varepsilon]}{\gamma} \end{Bmatrix} \quad (11)$$

As shown in Fig. 5, the superstructure nearly moves as a rigid body in the first mode shape  $\phi^1$ ; whereas in the second mode shape  $\phi^2$ , the displacements of the superstructure and the base isolator are opposite in direction.

If one normalizes the mode shapes of interstory drifts of the superstructure equal to 1. As shown in Fig. 6, with the aid of Eq. (10), then the mode shapes of the 2-DOF model can be given by

$$\phi^1 = \begin{Bmatrix} \frac{1 - \gamma\varepsilon}{\varepsilon} \\ 1 \end{Bmatrix}, \quad \phi^2 = \begin{Bmatrix} -\frac{\gamma(1 + \varepsilon)}{1 + \gamma\varepsilon} \\ 1 \end{Bmatrix} \quad (12)$$

The vector of equivalent story shear forces can be written, based on the theory of structural

Fig. 5(a) First mode shape of two-degree-of-freedom base isolation system (If  $\phi_b^1 = 1$ )Fig. 5(b) Second mode shape of two-degree-of-freedom base isolation system (If  $\phi_b^2 = 1$ )Fig. 6(a) First mode shape of two-degree-of-freedom base isolation system (If  $\phi_s^1 = 1$ )Fig. 6(b) Second mode shape of two-degree-of-freedom base isolation system (If  $\phi_s^2 = 1$ )

dynamics, as Tsai *et al.* (2003b), Chen (2003)

$$\mathbf{F} = \begin{Bmatrix} f_1 \\ f_2 \end{Bmatrix} = \sum_{n=1}^2 \omega_n^2 \mathbf{M} \Phi^n |q_n|_{\max}$$

$$= \omega_1^2 \begin{bmatrix} m + m_b & m \\ m & m \end{bmatrix} \begin{Bmatrix} \frac{1-\gamma\epsilon}{\epsilon} \\ 1 \end{Bmatrix} |q_1|_{\max} + \omega_2^2 \begin{bmatrix} m + m_b & m \\ m & m \end{bmatrix} \begin{Bmatrix} -\frac{\gamma(1+\epsilon)}{1+\gamma\epsilon} \\ 1 \end{Bmatrix} |q_2|_{\max}$$

$$\begin{aligned}
&= \begin{bmatrix} (m + m_b) \left( \omega_1^2 \left( \frac{1 - \gamma \varepsilon}{\varepsilon} \right) |q_1|_{\max} + \omega_2^2 \left( -\frac{\gamma(1 + \varepsilon)}{1 + \gamma \varepsilon} \right) |q_2|_{\max} \right) + m(\omega_1^2 |q_1|_{\max} + \omega_2^2 |q_2|_{\max}) \\ m \left( \omega_1^2 \left( \frac{1 - \gamma \varepsilon}{\varepsilon} \right) |q_1|_{\max} + \omega_2^2 \left( -\frac{\gamma(1 + \varepsilon)}{1 + \gamma \varepsilon} \right) |q_2|_{\max} \right) + m(\omega_1^2 |q_1|_{\max} + \omega_2^2 |q_2|_{\max}) \end{bmatrix} \\
&= \begin{bmatrix} (m + m_b)(C \omega_1^2 |q_1|_{\max} + D \omega_2^2 |q_2|_{\max}) + m(\omega_1^2 |q_1|_{\max} + \omega_2^2 |q_2|_{\max}) \\ m(C \omega_1^2 |q_1|_{\max} + D \omega_2^2 |q_2|_{\max}) + m(\omega_1^2 |q_1|_{\max} + \omega_2^2 |q_2|_{\max}) \end{bmatrix} \\
&= \begin{bmatrix} m_b(\omega_1^2 C |q_1|_{\max} + \omega_2^2 D |q_2|_{\max}) + m(\omega_1^2 |q_1|_{\max} (C + 1) + \omega_2^2 |q_2|_{\max} (D + 1)) \\ m(\omega_1^2 |q_1|_{\max} (C + 1) + \omega_2^2 |q_2|_{\max} (D + 1)) \end{bmatrix} \quad (13)
\end{aligned}$$

where

$$C = \frac{1 - \gamma \varepsilon}{\varepsilon} = \frac{1}{\varepsilon} - \gamma \approx \frac{1}{\varepsilon} \quad \left( \text{if } \gamma \ll \frac{1}{\varepsilon} \right) \quad (14)$$

and

$$D = -\frac{\gamma(1 + \varepsilon)}{1 + \gamma \varepsilon} \approx -\gamma[1 + (1 - \gamma)\varepsilon] \approx \frac{\gamma}{[1 - (1 - \gamma)\varepsilon]} \quad (\text{if } \varepsilon^2 \ll 1) \quad (15)$$

where  $f_1$  and  $f_2$  represent the base shear and story shear forces, respectively.

### 3. Rational design formulae for vertical distribution of lateral forces

In the UBC code, the lateral forces are assumed to be distributed over the height of the superstructure above the isolation interface in accordance with the formula (Uniform Building Code 1997, FEMA-273 1993, FEMA-274 1994):

$$F_x = V_s \frac{w_x h_x}{\sum_{i=1}^N w_i h_i} \quad (16)$$

$F_x$  represents the inertia force at level  $x$  above the isolation level;  $w_x$  and  $w_i$  represent the weight at level  $x$  and level  $i$ , respectively;  $h_x$ ,  $h_i$  are the heights of the  $x$ th and  $i$ th story above the isolation, respectively;  $V_s$  is the lateral seismic shear force;  $N$  is the total number of stories of the superstructure. The superstructure above the isolation system is designed and constructed to withstand a minimum shear force,  $V_s$ , using the formula

$$V_s = \frac{V_b}{R_l} = \frac{K_{D, \max} D_D}{R_l} \quad (17)$$

$V_b$  represents the design force for the superstructure and the elements below the isolation interface;  $D_D$  depicts the design displacement of base isolation;  $K_{D, \max}$  is the maximum effective stiffness of

the base isolator at the design displacement;  $R_I$  portrays the design force reduction factor (ductility factor), which is intended to account for the inelastic response in the superstructure.

It is evident that Eq. (16) leads to an inverted triangular vertical distribution of the inertia force over the height of the superstructure, as shown in Fig. 1. Furthermore, the inertia force on each floor above the base floor computed from Eq. (16) seems to be overestimated because the weight of the base floor is neglected. In view of this, Tsai *et al.* (2001a,b, 2002a, 2003a), have proposed two rational and simple design formulae for the vertical distributions of the lateral forces over the height of the superstructure while only considering the influence of the first mode of the base-isolated structure. The inertia force at each floor is given as (as shown in Fig. 5(a)) (Tsai *et al.* 2001a,b, 2002a, 2003a)

$$F_x = V_s \frac{w_x \left( 1 + \varepsilon \left( \frac{h_x}{H} \right) \right)}{\sum_{i=0}^N w_i \left( 1 + \varepsilon \left( \frac{h_i}{H} \right) \right)} \quad (18)$$

and

$$F_x = V_s \frac{w_x [1 + \varepsilon (\phi_s^1)_x^*]}{\sum_{i=0}^N w_i [1 + \varepsilon (\phi_s^1)_i^*]} \quad (19)$$

where  $\varepsilon = \omega_b^2 / \omega_s^2$  is the square of the ratio of natural frequencies, and also represents the ratio of the displacement at the top of superstructure relative to the base floor to that of the base floor (see Fig. 5(a));  $H$  represents the total height of the base-isolated structure above isolation level;  $(\phi_s^1)^*$  represents the first mode shape of the fixed-base structure (i.e., without any isolator);  $(\phi_s^1)_x^*$  and  $(\phi_s^1)_i^*$  describe the values of the first mode shape at level  $x$  and level  $i$ , respectively, when the superstructure is rigidly fixed. It should be noted that the value of the first mode shape at the top of the superstructure,  $(\phi_s^1)_N^*$ , should be normalized and equal to 1. The aforementioned two design formulae considering the influence of the first mode of the base-isolated structures have been proven by computational and experimental verification, and can accurately predict the lateral force distributions on isolated structures (Tsai *et al.* 2001a,b, 2002a, 2003a).

Moreover, if higher order terms of  $\varepsilon$  and  $\gamma\varepsilon$  value are considered (see Eq. (10)), Eqs. (18) and (19) can be rewritten as:

$$F_x = V_s \frac{w_x \left( 1 + \frac{\varepsilon}{1 - \gamma\varepsilon} \left( \frac{h_x}{H} \right) \right)}{\sum_{i=0}^N w_i \left( 1 + \frac{\varepsilon}{1 - \gamma\varepsilon} \left( \frac{h_i}{H} \right) \right)} \quad (20)$$

and

$$F_x = V_s \frac{w_x \left[ 1 + \frac{\varepsilon}{1 - \gamma\varepsilon} (\phi_s^1)_x^* \right]}{\sum_{i=0}^N w_i \left[ 1 + \frac{\varepsilon}{1 - \gamma\varepsilon} (\phi_s^1)_i^* \right]} \quad (21)$$



#### 4. Higher mode effects on vertical distributions of lateral forces

The aforementioned four design formulae can obtain satisfactory predictions of the vertical distribution of inertia forces under cases mostly restricted to the superstructures that are almost rigid body motions and that the frequencies of the first and second modes on isolated structures are well-separated. Up to now, no researcher has accounted for the contributions of higher modes to the lateral force distributions of base-isolated structures. To overcome these limitations, suitable vertical distribution formulae for inertia forces by considering the second mode contribution of a base-isolated structure are proposed in this paper. With the aid of Eq. (13), two design formulae are given as:

$$F_x = V_s \frac{w_x \left[ \omega_1^2 \left( \frac{1-\gamma\varepsilon}{\varepsilon} + \frac{h_x}{H} \right) + \omega_2^2 \frac{|q_2|_{\max}}{|q_1|_{\max}} \left( -\frac{\gamma(1+\varepsilon)}{1+\gamma\varepsilon} + \frac{h_x}{H} \right) \right]}{\sum_{i=0}^N w_i \left[ \omega_1^2 \left( \frac{1-\gamma\varepsilon}{\varepsilon} + \frac{h_i}{H} \right) + \omega_2^2 \frac{|q_2|_{\max}}{|q_1|_{\max}} \left( -\frac{\gamma(1+\varepsilon)}{1+\gamma\varepsilon} + \frac{h_i}{H} \right) \right]} \quad (22)$$

and

$$F_x = V_s \frac{w_x \left[ \omega_1^2 \left( \frac{1-\gamma\varepsilon}{\varepsilon} + (\phi_s^1)_x^* \right) + \omega_2^2 \frac{|q_2|_{\max}}{|q_1|_{\max}} \left( -\frac{\gamma(1+\varepsilon)}{1+\gamma\varepsilon} + (\phi_s^1)_x^* \right) \right]}{\sum_{i=0}^N w_i \left[ \omega_1^2 \left( \frac{1-\gamma\varepsilon}{\varepsilon} + (\phi_s^1)_i^* \right) + \omega_2^2 \frac{|q_2|_{\max}}{|q_1|_{\max}} \left( -\frac{\gamma(1+\varepsilon)}{1+\gamma\varepsilon} + (\phi_s^1)_i^* \right) \right]} \quad (23)$$

where the maximum values of  $q_1$  and  $q_2$  can be obtained by numerical analyses (Chopra 1995).

Moreover, in Eqs. (21) and (23), one presumes that the deflected shape of the superstructure relative to the base floor is the first mode shape  $(\phi_s^1)^*$  of the fixed-base structure (i.e., without any isolator). However, such satisfactory predictions are restricted to more regular structures. It is an important issue for an irregular structure to reasonably redistribute inertia forces on the superstructure by considering the contributions of higher modes on the superstructure (Chopra and Goel 2002). To overcome these limitations, several researchers have proposed adaptive force distributions to provide better estimates of the fixed-base structure (Chopra and Goel 2002, Jan *et al.* 2002). Chopra and Goel (2002) have developed an improved modal pushover analysis (MPA) procedure. Jan *et al.* (2002) have proposed an alternative method to simply estimate the lateral force distributions of high-rise buildings by combining contributions from the first and second modes. Based on proposed design formulae for the fixed-base structures by Chopra (1995), Chopra and Goel (2002) and Jan *et al.* (2002), one can combine the first- and second-mode contributions to obtain a distribution vector of the lateral force of the superstructure, and the distribution vector component is given as (Chopra 1995, Chopra and Goel 2002, Jan *et al.* 2002):

$$\alpha_x = \frac{\omega_{s1}^2 w_x (\phi_s^1)_x^* + \omega_{s2}^2 \frac{|q_2|_{\max}}{|q_1|_{\max}} w_x (\phi_s^2)_x^*}{\omega_{s1}^2 w_N (\phi_s^1)_N^* + \omega_{s2}^2 \frac{|q_2|_{\max}}{|q_1|_{\max}} w_N (\phi_s^2)_N^*}, \quad (x = 1 \text{ to } N) \quad (24)$$

where  $\omega_{s1}$  and  $\omega_{s2}$  depict the first- and second-mode natural frequencies of the fixed-base structure, respectively;  $w_x$  and  $w_N$  describe the weight at level  $x$  and level  $N$ , respectively;  $(\phi_s^1)_x^*$  and  $(\phi_s^2)_x^*$

represent the first- and second-mode shapes of the fixed-base structure at level  $x$ , respectively;  $(\phi_s^1)_N^*$  and  $(\phi_s^2)_N^*$  are the first- and second-mode shapes of the fixed-base structure at level  $N$  and are normalized to 1. It should be noted that the value of the vector component at the roof level,  $\alpha_N$ , should be equal to 1; and

$$\frac{|q_2^*|_{\max}}{|q_1^*|_{\max}} = \frac{|\Gamma_2 D_2(\omega_{s2}, \xi_2)|}{|\Gamma_1 D_1(\omega_{s1}, \xi_1)|} \quad (25)$$

where the  $n$ th-mode participation factor,  $\Gamma_n$ , is given by (Chopra 1995, Chopra and Goel 2002, Jan *et al.* 2002)

$$\Gamma_n = \frac{(\phi_s^n)^{*T} \mathbf{m} \mathbf{v}}{(\phi_s^n)^{*T} \mathbf{m} (\phi_s^n)^*} \quad (26)$$

where  $(\phi_s^n)^*$  indicates the  $n$ th-mode shape of the fixed-base structure;  $\mathbf{m}$  represents the mass matrix of the fixed-base structure;  $D_n$  represents the  $n$ th-mode spectral displacement;  $\xi_n$  denotes the  $n$ th-mode damping ratio of the fixed-base structure;  $\mathbf{v}$  depicts the influence vector.

If one only considers the influence of the first mode of the base-isolated structure and simultaneously considers the first- and second-mode contributions of the superstructure, the design formula is given as:

$$F_x = V_s \frac{w_x \left[ \frac{1 - \gamma \varepsilon}{\varepsilon} + \alpha_x \right]}{\sum_{i=0}^N w_i \left[ \frac{1 - \gamma \varepsilon}{\varepsilon} + \alpha_i \right]} \quad (27)$$

Besides, to obtain more accurate results, one can take into account the influence of the second mode of the base-isolated structure and the higher mode contributions of the superstructure, and the design formula can be expressed as:

$$F_x = V_s \frac{w_x \left[ \omega_1^2 \left( \frac{1 - \gamma \varepsilon}{\varepsilon} + \alpha_x \right) + \omega_2^2 \frac{|q_2|_{\max}}{|q_1|_{\max}} \left( -\frac{\gamma(1 + \varepsilon)}{1 + \gamma \varepsilon} + \alpha_x \right) \right]}{\sum_{i=0}^N w_i \left[ \omega_1^2 \left( \frac{1 - \gamma \varepsilon}{\varepsilon} + \alpha_i \right) + \omega_2^2 \frac{|q_2|_{\max}}{|q_1|_{\max}} \left( -\frac{\gamma(1 + \varepsilon)}{1 + \gamma \varepsilon} + \alpha_i \right) \right]} \quad (28)$$

## 5. Experimental verification for a multiple-bay base-isolated structure

In order to verify the accuracy and suitability of proposed design formulae considering higher mode contributions of the isolated structure, a series of shaking table tests of a multiple-bay isolated structure were carried out, and given as an example to investigate the distinction among these proposed design formulae, the UBC code provision, and experimental results. As shown in Figs. 7 to 9, a 40% scale three-story base-isolated steel structure is constructed as a moment-resisting frame. The structure used for mounting base isolators is rectangular in shape, rising 4.25 m vertically and occupying a plane of 4.5 m  $\times$  4 m horizontally. The weights from the base floor to the roof were approximately estimated equal to 108, 93, 93, and 85 kN, respectively.

The isolation system was composed of five natural rubber bearings (NRB) and four stirrup rubber

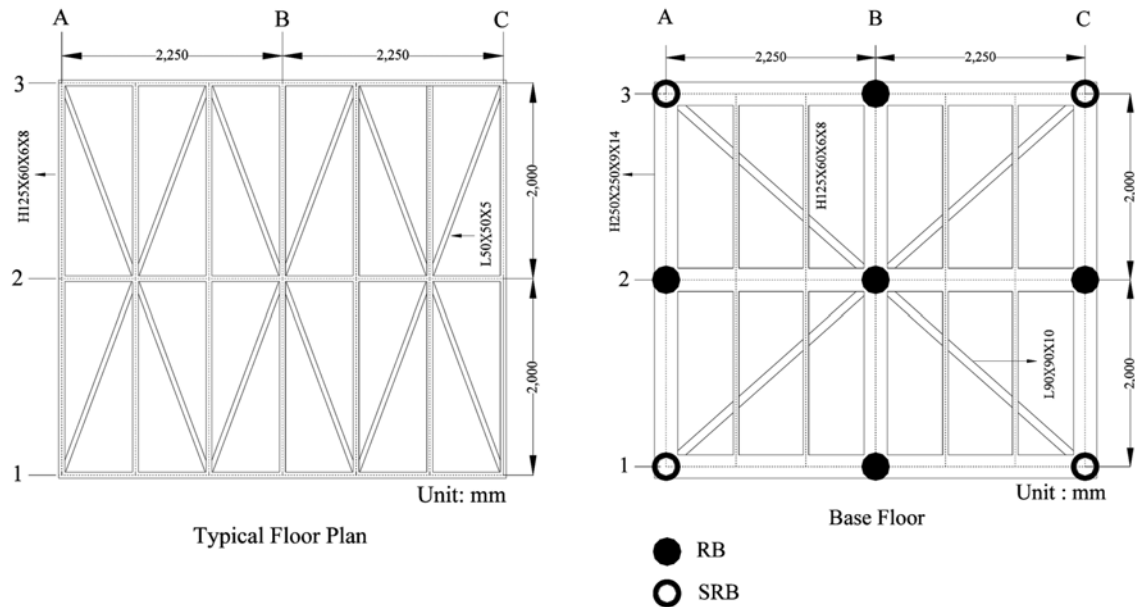


Fig. 7 Typical plan of test base-isolated structure

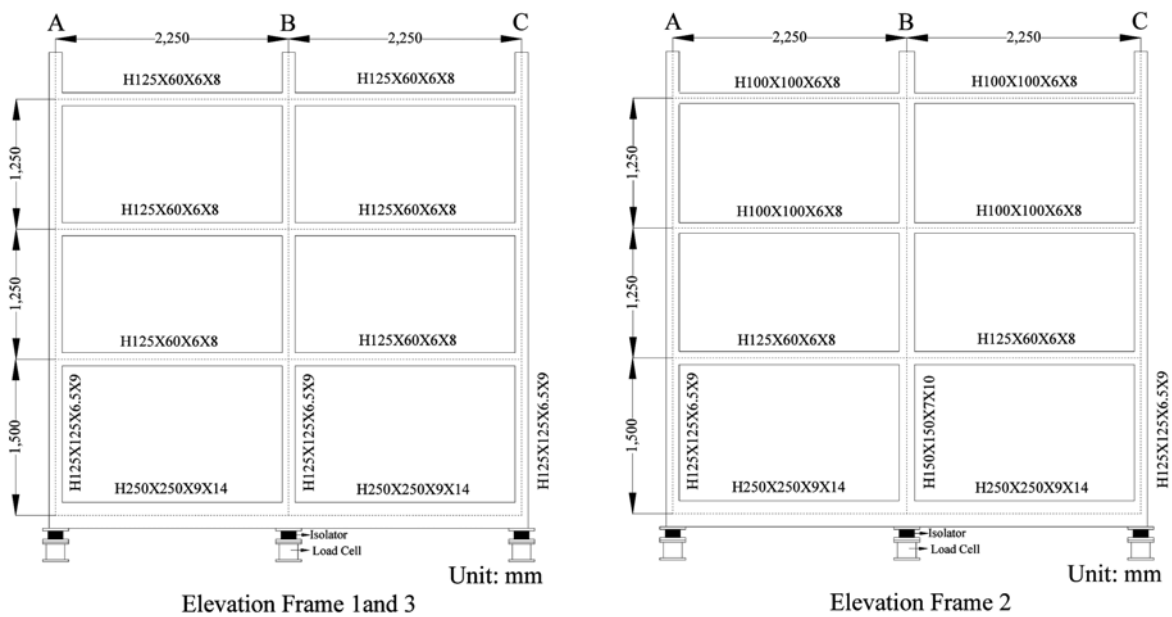


Fig. 8 Longitudinal direction elevation of test base-isolated structure

bearings (SRB) (Tsai *et al.* 2002b), as shown in Fig. 7. Fig. 10 shows that the type of natural rubber bearings tested is 146 mm in diameter and 84 mm in height. They consist of 10 rubber layers of 5 mm thickness each, 9 steel plates of 1 mm thickness each and 3 mm rubber cover, and each end plate is 12.5 mm thick with bolted connections. Fig. 11 shows that the type of stirrup rubber bearing (noted as SRB) tested is also 146 mm in diameter and 84 mm in height. Each bearing consists of a

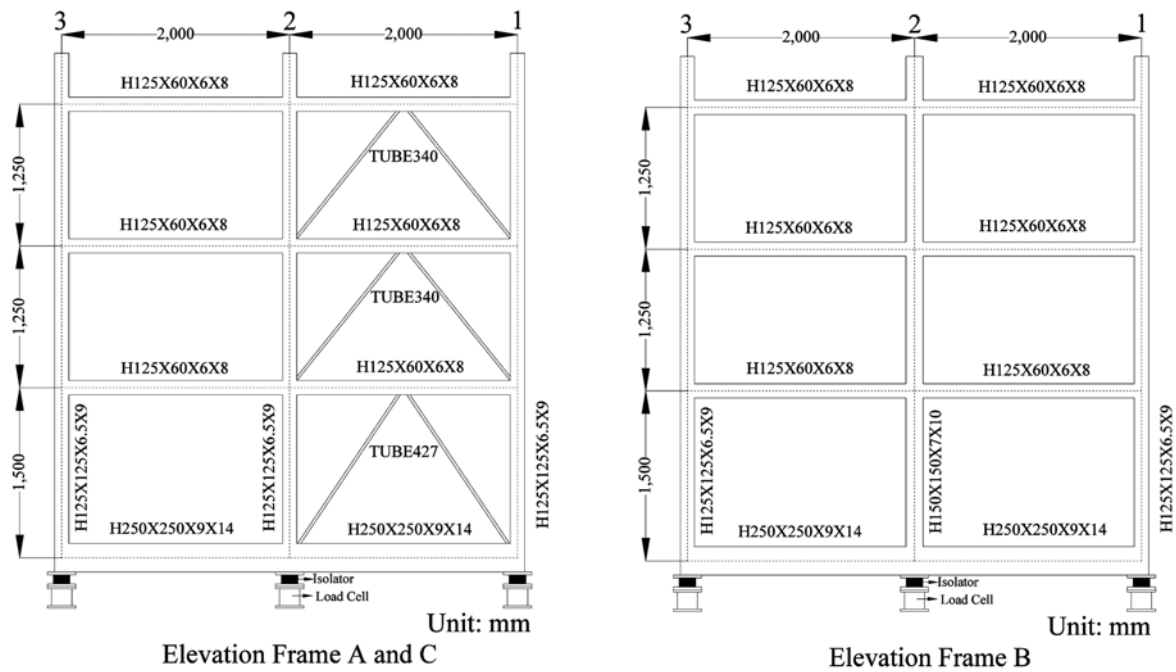


Fig. 9 Transverse direction elevation of test base-isolated structure

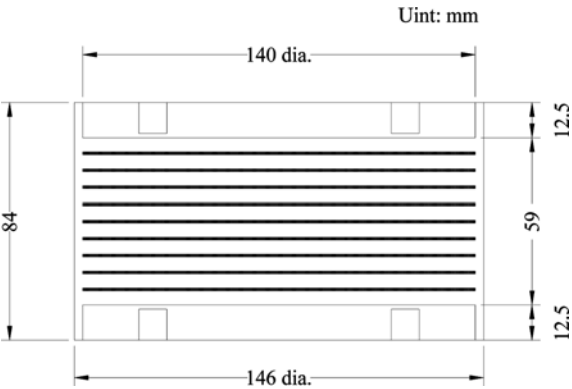


Fig. 10 Schematic of natural rubber bearing (NRB)

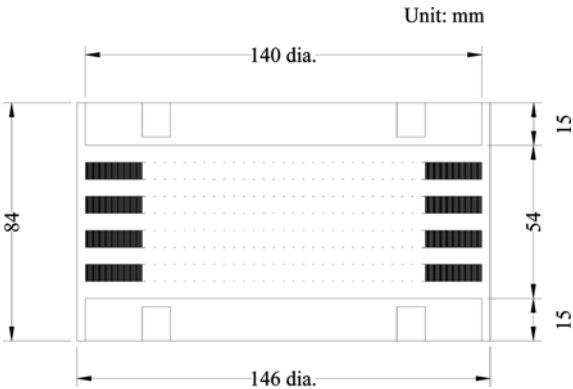


Fig. 11 Schematic of stirrup rubber bearing (SRB)

lump of rubber materials of 54 mm in thickness, 4 external steel rings of 6 mm, 3 mm rubber cover, and a plate of 15 mm thickness at each end with bolted connections. The SRB bearing research conducted by Tsai in Taiwan (2002b), experimental examinations via the component and shaking table tests, indicate that the SRB bearing possesses higher damping ratios at higher strains, and lower horizontal effective stiffness than other kinds of rubber bearings even when the vertical axial load is slight.

The base-isolated structure was subjected to the 1940 El Centro and the 1994 Northridge (New Hall) earthquakes in U. S. A., the 1995 Kobe earthquake in Japan, and the 1999 Chi-Chi (TCU129) earthquake in Taiwan. Table 1 lists test results conducted in the longitudinal direction of the base-

Table 1 List of earthquake simulation tests conducted in longitudinal direction of a multiple-bay base-isolated structure

Test No.	Input earthquake	Direction	PGA (g)
1	Chi-Chi (TCU129)	EW	1.022
2	El Centro	NS	0.601
3	Kobe	EW	0.701
4	Northridge (New Hall)	NS	0.317

Table 2 Prototype mode shapes for fixed base steel structure

Longitudinal direction		
Floor	First mode shape	Second mode shape
Roof	1.000	1.000
2F	0.754	-0.306
1F	0.442	-1.021

Table 3  $\varepsilon$  Values in shaking table tests

Earthquake	$\varepsilon$
Chi-Chi (TCU129) (PGA = 1.022 g)	0.146
El Centro (PGA = 0.601 g)	0.113
Kobe (PGA = 0.701 g)	0.138
Northridge (New Hall) (PGA = 0.317 g)	0.142

isolated structure. The first two natural frequencies are 2.91 Hz and 11.91 Hz in the longitudinal direction of the structure without isolators. The mode shapes of the multiple-bay steel structure without isolators are shown in Table 2. The mass ratio  $\gamma (= m/M)$  is equal to 0.714. In this study, the main goal of experiments is to probe into the vertical distribution of lateral forces and verify the new proposed design formulae in comparison with the UBC code provision. Therefore, the design force reduction factor  $R_f$  is not included (i.e.,  $R_f=1$ ) in this study.

Table 3 exhibits the magnitude of the  $\varepsilon (= \omega_b^2/\omega_s^2)$  value through the shaking table test. It was computed based on the experimental first mode frequency of the fixed-base structure and the base-isolated structure during different earthquake simulation tests. It shows the effectiveness of the rubber bearings mounted on this three-floor steel frame. Table 4 represents the magnitudes of the  $|q_2|_{\max}/|q_1|_{\max}$  of Eqs. (22) and (23) and  $|q_2^*|_{\max}/|q_1^*|_{\max}$  of Eq. (24) values through numerical analyses. It represents the second-mode contributions of the base-isolated and fixed-base structures, respectively. Table 5 exhibits lateral force distribution vector components  $\alpha_x$  at each floor for the fixed-base steel structure during different ground motions.

In order to reasonably compare the experimental results and computational results, the base shears were obtained based on the summations of the inertia force at each floor through the shaking table

Table 4  $\frac{|q_2|_{\max}}{|q_1|_{\max}}$  and  $\frac{|q_2^*|_{\max}}{|q_1^*|_{\max}}$  values from numerical analyses

Earthquake	$\frac{ q_2 _{\max}}{ q_1 _{\max}}$	$\frac{ q_2^* _{\max}}{ q_1^* _{\max}}$
Chi-Chi (TCU129) (PGA = 1.022 g)	0.020	0.045
El Centro (PGA = 0.601 g)	0.014	0.019
Kobe (PGA = 0.701 g)	0.016	0.039
Northridge (New Hall) (PGA = 0.317 g)	0.010	0.031

Table 5 Lateral force distribution vector components  $\alpha_x$  at each floor for longitudinal direction of fixed-base steel structure

	TCU129	El Centro	Kobe	New Hall
Roof	1.000	1.000	1.000	1.000
2F	0.328	0.547	0.369	0.428
1F	-0.207	0.097	-0.150	-0.067

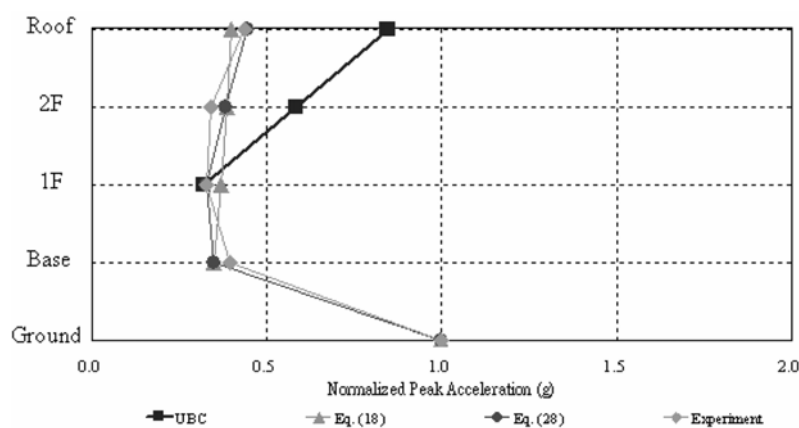


Fig. 12 Comparisons of normalized peak story accelerations of multiple-bay isolated steel structure under Chi-Chi (TCU129) earthquake

tests. Figs. 12 to 15 depict the normalized peak accelerations on each floor calculated by Eqs. (18) and (28), the formula provided by the UBC code, and experimental results through shaking table tests. The computationally normalized peak accelerations on each floor were obtained by dividing the inertia forces by the corresponding masses times the peak ground accelerations. From these figures, it proves that results obtained from proposed design formulae are in good agreement with the experimental results. Moreover, it will be more accurate by considering higher mode effects of the base-isolated structure and the superstructure. It is also illustrated that will overestimate the maximum absolute acceleration on higher floors in the UBC code.

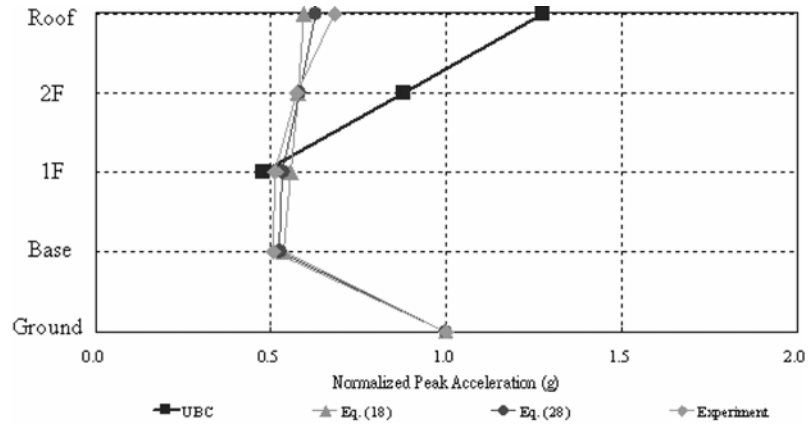


Fig. 13 Comparisons of normalized peak story accelerations of multiple-bay isolated steel structure under El Centro earthquake

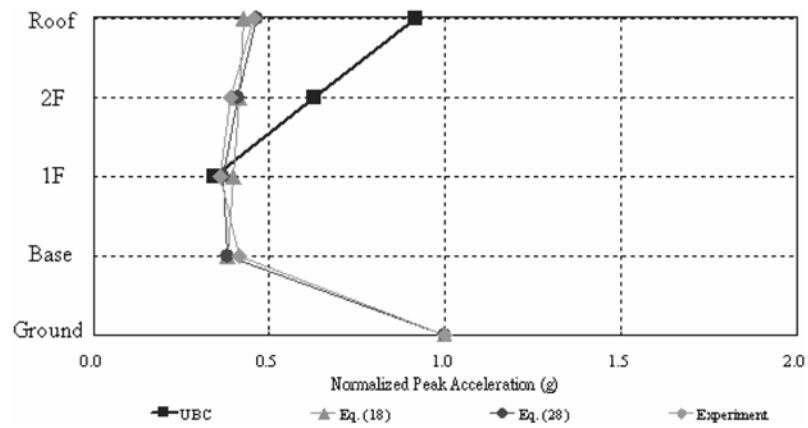


Fig. 14 Comparisons of normalized peak story accelerations of multiple-bay isolated steel structure under Kobe earthquake

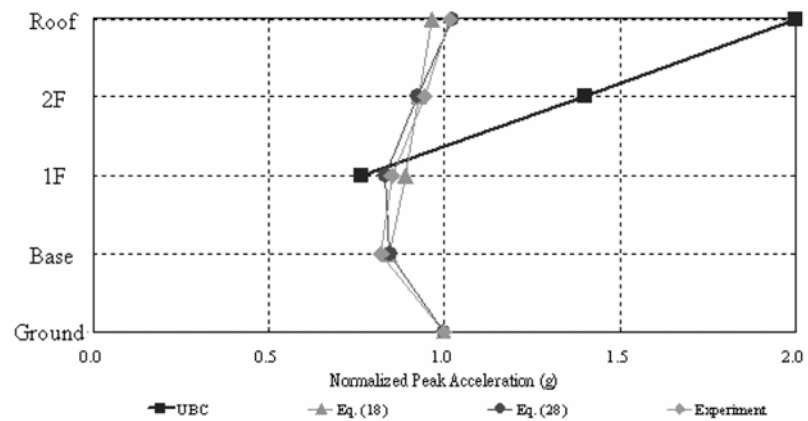


Fig. 15 Comparisons of normalized peak story accelerations of multiple-bay isolated steel structure under Northridge (New Hall) earthquake

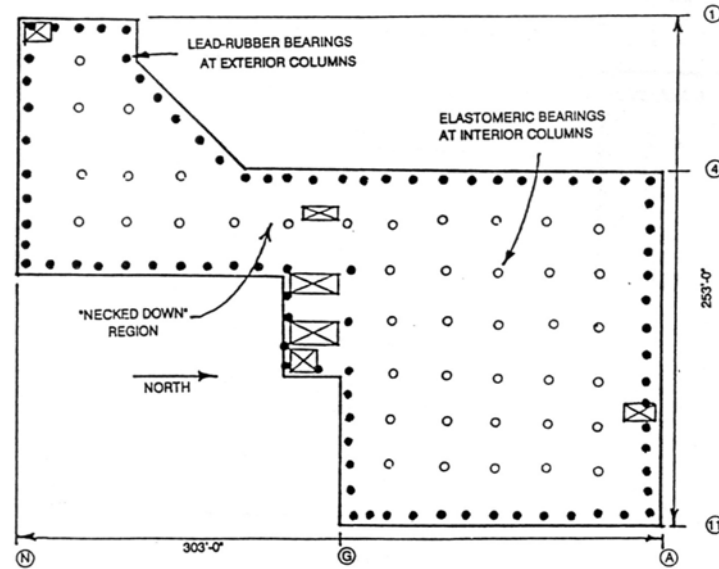


Fig. 16 USC University Hospital floor plan

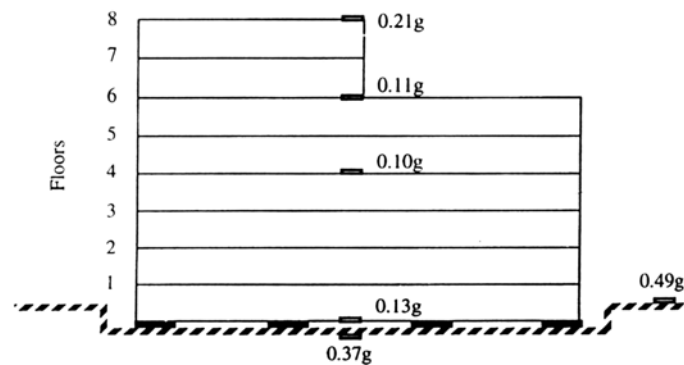


Fig. 17 Recorded floor accelerations of USC University Hospital

## 6. Verification of proposed formulae through recorded data

In addition to the experimental verification, recorded floor accelerations for the University Hospital of the University of Southern California during the 1994 Northridge earthquake, as shown in Figs. 16 and 17 (Asher *et al.* 1990, Komodromos 2000), are adopted to investigate distinctions among the proposed design formulae, UBC code provision, and recorded data. The USC University Hospital is an eight-story, steel braced frame structure that is seismically isolated on a combination of 68 lead-rubber and 81 elastomeric bearings at the University of California Medical Campus (Asher *et al.* 1990). Significant higher mode effects on seismic responses are expected during earthquakes due to its irregular geometry. It is the world's first base-isolated hospital. It is also the first base-isolated building in the United States that has experienced a significant earthquake ground motion during the 1994 Northridge earthquake. Fig. 17 shows the recorded peak accelerations of the



Table 6 Prototype mode shape for north-south direction of fixed-base USC University Hospital

Floor	First mode shape	Second mode shape
Roof	1.000	1.000
7F	0.791	0.235
6F	0.568	-0.508
5F	0.350	-1.026
4F	0.188	-1.105
3F	0.132	-0.955
2F	0.085	-0.691
1F	0.040	-0.357

Table 7 Lateral force distribution vector components  $\alpha_x$  of each floor for north-south direction of fixed-base USC University Hospital

Floor	$\alpha_x$
Roof	1.000
7F	0.418
6F	0.030
5F	-0.371
4F	-0.508
3F	-0.461
2F	-0.376
1F	-0.214

ground and certain floors of the USC University Hospital in the north-south direction (Komodromos 2000). The peak free-field and peak foundation accelerations in the north-south direction were 0.49 g and 0.37 g, respectively. The maximum floor accelerations were recorded at the base and the roof of the hospital to be 0.13 g and 0.21 g, respectively. The peak floor accelerations were also recorded at the 4th floor and 6th floor to be 0.10 g and 0.11 g, respectively. In this study, linear interpolation is utilized to obtain other floor accelerations without instrumentation. The mass from the base floor to the roof were equal to 33.275, 14.874, 13.709, 12.354, 12.233, 12.146, 9.769, 8.897, 10.942 slugs, respectively. The first two natural frequencies are approximately 1.93 Hz and 4Hz in the north-south direction of the fixed-base USC University Hospital. The mode shapes of the fixed-base hospital are shown in Table 6.

The mass ratio  $\gamma (=m/M)$  is equal to 0.74, and the magnitude of the  $\varepsilon (= \omega_b^2 / \omega_s^2)$  value is equal to 0.15. The magnitudes of the  $|q_2|_{\max} / |q_1|_{\max}$  and  $|q_2^*|_{\max} / |q_1^*|_{\max}$  values are 0.0317 and 0.2290, respectively. Table 7 displays the lateral force distribution vector components  $\alpha_x$  at each floor for the fixed-base case. Table 8 exhibits the comparisons of results calculated from the UBC code provision, the proposed design formulae, and the recorded acceleration data in the north-south direction of the USC University Hospital. It is illustrated that the vertical distributions of peak accelerations computed by proposed design formulae are in good agreement with the recorded floor accelerations. Fig. 18 illustrates the normalized peak accelerations on each floor calculated by Eqs. (18) and (28), the formula provided by the UBC code, and the recorded acceleration data. It demonstrates that the proposed design formulae can well predict the vertical distributions of peak

Table 8 Acceleration comparisons of results obtained from proposed design formulae, UBC code provision, and recorded acceleration data in north-south direction of USC University Hospital during ground motions

	Base	1F	2F	3F	4F	5F	6F	7F	8F
Equation (18)	0.120	0.122	0.124	0.126	0.129	0.131	0.133	0.136	0.138
Equation (19)	0.122	0.123	0.123	0.124	0.125	0.128	0.132	0.137	0.141
Equation (20)	0.118	0.121	0.124	0.126	0.129	0.132	0.135	0.137	0.140
Equation (21)	0.121	0.122	0.123	0.124	0.125	0.129	0.133	0.138	0.143
Equation (22)	0.110	0.115	0.121	0.126	0.132	0.137	0.143	0.148	0.154
Equation (23)	0.115	0.117	0.119	0.121	0.123	0.131	0.141	0.151	0.161
Equation (27)	0.128	0.124	0.120	0.118	0.117	0.120	0.129	0.138	0.151
Equation (28)	0.131	0.119	0.111	0.107	0.104	0.111	0.132	0.153	0.183
UBC Code	N/A	0.041	0.082	0.123	0.163	0.204	0.245	0.286	0.327
Recorded Data	0.130	0.122	0.115	0.109	0.104	0.105	0.106	0.149	0.205

Units: g

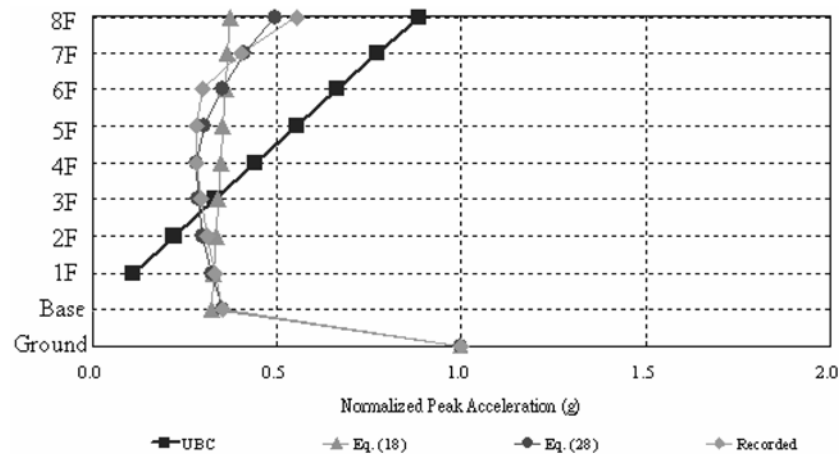


Fig. 18 Comparisons of normalized peak story accelerations of USC University Hospital under 1994 Northridge earthquake

accelerations in actual earthquakes. When the higher mode effect is considered, better agreement with the recorded data is observed. Furthermore, it also demonstrates that the acceleration at each floor calculated by the UBC code provision has been found to be remarkably distinct in contrast with the recorded acceleration data and too conservative.

## 7. Conclusions

The design of seismically isolated structures is mainly governed by the Uniform Building Code (UBC) published by the International Conference of Building Officials. Nevertheless, the vertical distribution of lateral forces over the height of the superstructure in the UBC code provision is on the basis of an inverted triangular force distribution. It has been found to bound responses of most

isolated structures conservatively, even when higher mode contributions are generated. The design formulae proposed in this paper can reasonably incorporate the influence of the inertial force on the base floor to accurately calculate the lateral force distributions on isolated structures via the verification of the experimental and recorded data. Meanwhile, the proposed design formulae considering higher mode effects are in good agreement with the actual vertical distributions of lateral forces on base-isolated structures.

## Acknowledgements

Special thanks is given to the National Science Council, Taiwan, R. O. C., for financial support for this research (NSC 90-2211-E-035-016). The assistance from the National Center for Research on Earthquake Engineering in Taiwan and KPFF Consulting Engineerings in U. S. A. are appreciated.

## References

- Asher, Jefferson W., Van Volkinburg, David R., Mayes, Ronald L., Kelly, Trevor, Sveinsson, Bjorn I and Hussain, Saif (1990), "Seismic isolation design of the USC University Hospital", *Proc. of Fourth U.S. Nat. Conf. on Earthquake Engineering*, Palm Springs, California, U. S. A., 3, May.
- Chen, Bo-Jen (2003), "Characteristics and earthquake-proof benefits of rubber bearings", Ph. D. Dissertation, Feng Chia University, Taiwan, R. O. C.
- Chopra, Anil K. (1995), *Dynamics of Structures: Theory and Applications to Earthquake Engineering*, Prentice-Hall, Inc.
- Chopra, Anil K. and Goel, Rakesh K. (2002), "A modal pushover analysis procedure for estimating seismic demands for buildings", *Earthq. Eng. Struct. Dyn.*, **31**, 561-582.
- Jan, T.S., Liu, M.W. and Kao, Y.C. (2002), "Pushover analysis and seismic of structures to near fault earthquake", A Research Report of National Council of Taiwan, Report No: NSC 90-2211-E-035-014, Sept.
- Kelly, James M. (1997), *Earthquake-Resistant Design with Rubber*, Second Edition, Springer-Verlag, London.
- Kelly, James M. (1999), "The role of damping in seismic isolation", *Earthq. Eng. Struct. Dyn.*, **28**, 3-20.
- Komodromos, Petros (2000), *Seismic Isolation for Earthquake-Resistant Structures*, WIT Press, Southampton, Boston.
- Lee, D.G., Hong, J.M. and Kim, J. (2001), "Vertical distribution of equivalent static loads for base isolated building structures", *Eng. Struct.*, **23**, 1293-1306.
- Naeim, Farzad and Kelly, James M. (1999), *Design of Seismic Isolated Structures: From Theory To Practice*, John Wiley & Sons, Inc.
- NEHRP Guidelines for the Seismic Rehabilitation of Buildings, Federal Emergency Management Agency, FEMA-273, 1993.
- NEHRP Guidelines for the Seismic Rehabilitation of Buildings, Federal Emergency Management Agency, FEMA-274, 1994.
- Tsai, C.S., Chen, Bo-Jen and Chiang, Tsu-Cheng (2001a), "Reasonable formulae of lateral force distributions for base-isolated structures", *J. Civil Eng. Tech.*, **5**(1), 49-67, March, (in Chinese).
- Tsai, C.S., Chen, Bo-Jen, Chiang, Tsu-Cheng and Chen, Ching-Shyang (2001b), "Assessment of applications of rubber bearings to seismic retrofit of essential structures", *2001 First Int. Conf. on Planning and Design, National Cheng Kung University*, Tainan, Taiwan, R. O. C.
- Tsai, C.S., Chen, Bo-Jen and Chiang, Tsu-Cheng (2002a), "Reasonable lateral force distributions on isolated structures", *The 2002 ASME Pressure Vessels and Piping Conf., Seismic Engineering 2002*, Vancouver, British Columbia, Canada, **2**, 229-236, August.

- Tsai, C.S., Chen, Bo-Jen and Chiang, Tsu-Cheng (2002b), "Shaking table tests of full scale base-isolated structures", *The 2002 ASME Pressure Vessels and Piping Conf.*, Vancouver, British Columbia, Canada, **2**, 245-252, August.
- Tsai, C.S., Chen, Bo-Jen and Chiang, Tsu-Cheng (2003a), "Experimental and computational verification of reasonable design formulae for base-isolated structures", *Earthq. Eng. Struct. Dyn.*, **32**, 1389-1406.
- Tsai, C.S., Chen, Bo-Jen, Chiang, Tsu-Cheng and Pong, Wen-Shen (2003b), "Verification of lateral force distributions for base-isolated structures including higher mode effects", *The 2003 ASME Pressure Vessels and Piping Conf.*, Cleveland, U. S. A., 65-72, July.
- Uniform Building Code (1997), *International Conference of Building Officials*, Whilter, California.